A New Soft X-Ray Polarimeter and Ellipsometer at BL-11

T. Imazono,[1] K. Sano,[2] Y. Suzuki,[1] T. Kawachi,[1] and M. Koike[1]

Abstract

A novel apparatus for polarimetric and ellipsometric measurements in the soft x-ray (SX) region has been designed, constructed, and installed in BL-11. It can realize the optical configurations for the complete polarization analysis based on the rotating-analyzer ellipsometry by using six independently movable drive shafts. As the performance test of the apparatus, linear polarization measurement has been demonstrated using two identical Mo/Si multilayer mirrors (period: 10.36 nm, ratio of thickness of Mo layer to period: 0.64, and 23 bilayers with topmost Si layer) deposited on the surface of commercial Si(111) substrates by an ion beam sputtering technique as reflection-type polarizers. The incident wavelength was scanned from 12.4 nm to 14.8 nm by a Monk-Gillieson type varied-line-spacing plane grating monochromator of BL-11, and the angles of incidence of both polarizers were also varied from 37.5° to 52.3°. The polarizances depend strongly on the incident wavelength, and the best performance of over 99% has been obtained at the wavelength of 13.9 nm. Furthermore, the degree of linear polarization of BL-11 has been assessed to be 85-88% in the measured wavelength range for the first time since the completion of the beamline. This means that BL-11 is upgraded as the comprehensive evaluation beamline for optical elements including polarizing elements for use in the SX region.

---

[1] *Quantum Beam Science Directorate, Japan Atomic Energy Agency, 8-1-7 Umemidai, Kizugawa, Kyoto 619-0215, Japan*

[2] *Shimadzu Emit Co. Ltd., 2-5-23 Kitahama, Chuo-ku, Osaka 541-0041, Japan*

1. Introduction

A phase shifter (or phase shifting polarizer) and analyzer are indispensable for the quantitative evaluation of the polarization state of light. In the vacuum-ultraviolet region, it has been successfully done with a reflection polarimeter equipped with Au- and Pt-coated mirrors as the phase shifter and analyzer, respectively.[1] In the soft x-ray (SX) range up to the water-window region (284-530 eV), a variety of multilayers, e.g., Mo/Si (~100 eV), Cr/C (~300 eV), and Sc/Cr (~400 eV), have been developed and utilized for polarimetric or ellipsometric measurements.[2] Most recently a multilayer-type phase shifter made of W/B_4C has been developed and polarization analysis of an undulator light source between 640 eV and 850 eV has been performed successfully.[3] This is the first report on the full characterization of the polarization state in the energy range of the *L* absorption edges of Fe, Co, and Ni by means of a multilayer phase shifter. In the energy region higher than 6 keV, single crystals, e.g., Si, Ge, and diamond in Bragg or Laue geometry have been utilized for the evaluation and generation of linearly and circularly polarized x-rays, and helicity switching.[4] Unfortunately, in the energy range between ~1 keV and 6 keV, it is difficult to develop practical phase shifters or even polarizers, and consequently to perform polarization measurements.

In our previous study, a mica crystal has been showed to work as a high-efficiency polarizer at 880 eV [5, 6] and the linear polarization degree of the light emerging from an undulator has been evaluated by using a versatile apparatus for polarimetry and ellipsometry (ELLI) [7] equipped with mica crystals as the polarizers. Furthermore, it has been found theoretically that mica film of ~5 μm thickness is a promising candidate as a transmission quarter-wave plate at around 1 keV.[8] This means that, in principle, it allows us to determine all of the polarization parameters of light in this energy region. As a part of the effort to certify these features, we have developed a new soft x-ray polarimeter and ellipsometer (SXPE) for complete polarization analysis after the model of ELLI.[9, 10] SXPE was installed in the evaluation beamline for SX optical elements (BL-11) [11] at AURORA, a superconducting compact storage ring,[12] of SR Center, Ritsumeikan University.

In this paper, we describe briefly the rotating-analyzer method with a phase shifter to realize the complete polarization analysis [13] in the next section. The design and construction of the new apparatus are dealt in Section 3. In Section 4, a Mo/Si multilayer mirror fabricated for the use of the performance test of the apparatus is described. In Sections 5 and 6, experimental set-up and result of the polarization measurement are represented, respectively. In the performance test, we describe a comparison of reflection profiles of the Mo/Si multilayer mirrors in the vicinity of *L*-absorption edge of Si measured by the new apparatus and an existing conventional reflectometer, and then perform linear polarization measurement in the wavelength range from 12.4 nm to 14.8 nm. Consequently the value of the linear polarization degree of BL-11 is showed for the first time since the completion of the beamline. [14]

2. Rotating-analyzer ellipsometry with a phase shifter

Rotating-analyzer ellipsometry by means of an analyzer A and a detector D is one of the well-known and simple polarization measurements as shown in Fig. 1(a). When the azimuth angle η is rotated along the optical axis of a probe beam fixing the incident angle ω and the detection angle θ, the intensity $I(\eta)$ of the reflected light from A follows the modified Malus' equation expressed as

$$I(\eta) = I_a\left(1 + C\cos 2(\eta - \delta)\right), \tag{1}$$

where I_a is the average of the maximum $I_{\max}$ and minimum $I_{\min}$ of the reflected light, δ is the azimuth angle of the major axis of the polarization ellipse of the incident light, and C is the contrast factor of the incident light defined as

$$C = \left(I_{\max} - I_{\min}\right)/\left(I_{\max} + I_{\min}\right). \tag{2}$$

We can obtain C and δ by applying the fitting function Eq. (1) to the measured data. The polarizance Z, which represents the polarizing ability of the analyzer, is defined using the reflectivities for s- and p-polarization components (R_s and R_p) of A as

$$Z = \left(R_s - R_p\right)/\left(R_s + R_p\right). \tag{3}$$

If the value of Z is given in advance, the degree of linear polarization P_L can be derived from

$$P_L = C/Z\,. \tag{4}$$

If the incident light is completely unpolarized or circularly polarized light as well as Z equals zero, then $I(\eta)$ is independent of η, so that P_L cannot be determined. Thus, when both Z and P_L are unknown, another polarizer (or a phase shifter) is needed.

Figure 1(c) shows a double-reflection geometry using both a polarizer (or a phase shifter), P, and an analyzer, A. The contrast factor of the reflected beam from P fixed at the azimuth angle $\chi = \delta \pm \pi/4$ is obtained by azimuth rotation of η, then P_L can be derived from

$$P_L = \left(C_1 C_2 / C_3 \cos 2\eta_3\right)^{1/2}, \tag{5}$$

where C_1 (or C_2) is the contrast factor of the incident beam evaluated by A (or P) in the configuration in Fig. 1(a) (or Fig. 1(b)). Also C_3 and η_3 are the contrast factor and the azimuth angle of the major axis of the polarization ellipse of the reflected beam from P in the configuration in Fig. 1(c), respectively. The above scheme makes it possible to determine

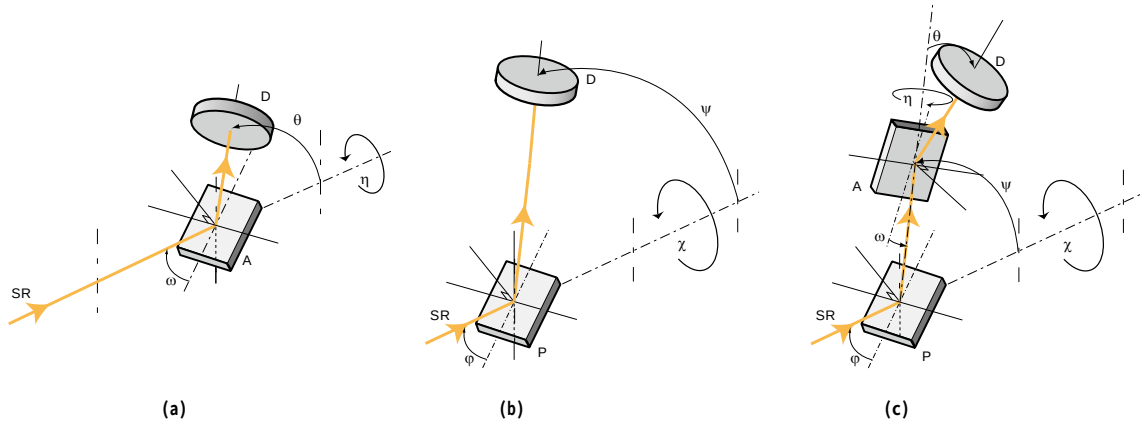

Figure 1 Three optical configurations for the polarization measurement based on rotating-analyzer ellipsometry using a reflection phase shifter (or polarizer) P and analyzer A. D represents a detector. They show a single-reflection geometry with A (a), a single-reflection geometry with P (b), and a double-reflection geometry with both P and A (c). The azimuth and incident angles of P (or A) are χ (or η) and φ (or ω), respectively. θ means a detection angle. ψ moves the position of A and D with those relative positions fixed.

simultaneously Z_i (i = 1, 2) of A and P, and P_L and δ of the incident light by using Eqs. (4) and (5).

If some pairs of (η_3, χ) are obtained by the measurements in the configuration shown in Fig. 1(b), then the polarization degree P and the ellipticity angle ε of light, and the extinction ratio ρ defined as the ratio of the complex amplitude for s-polarization to that for p-polarization and the phase difference Δ between s- and p-polarization components of P can be determined as fitting parameters by the following equation: [13]

$$\tan 2\eta_3 = \frac{2\rho P\left(\cos 2\varepsilon \cos\Delta \sin 2(\delta-\chi) - \sin 2\varepsilon \sin\Delta\right)}{\rho^2 - 1 + P\left(\rho^2+1\right)\cos 2\varepsilon \cos 2(\delta-\chi)}. \tag{6}$$

The degree of circular polarization P_C can be derived from

$$P_C = P \sin 2\varepsilon\,. \tag{7}$$

It is of importance that the polarization state of the incident light and the characteristics of two

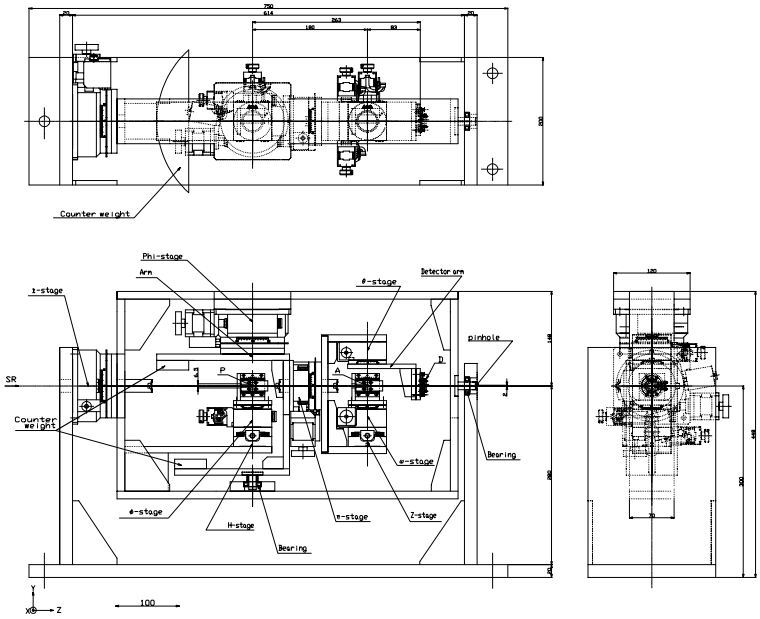

(a)

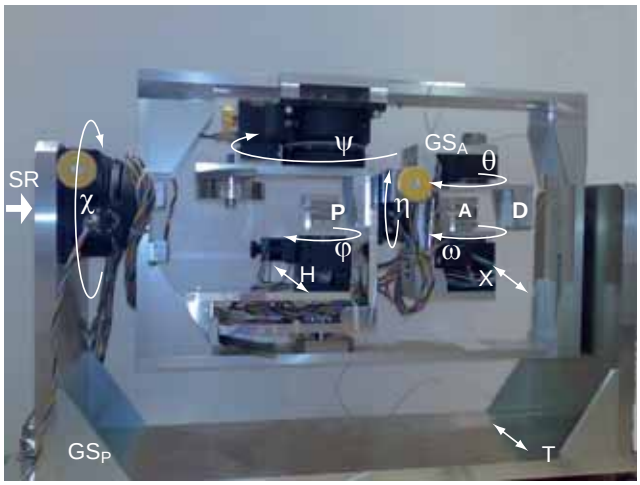

(b)

(c)

Figure 2 Projection drawing (a) and photograph (b) of the internal mechanism, and photograph of the vacuum chamber (c), of SXPE. Two goniometric stages GS_P and GS_A are equipped to mount a phase shifter (or polarizer) P and an analyzer A, respectively. Six motorized rotary stages (χ, φ, ψ, η, ω, and θ) and three motorized linear stages (H, X, and T) are employed to realize the configurations in Fig. 1 and to move the positions of P, A, and the internal mechanism itself in the x direction, respectively. In this figure T-stage located under the U-shaped basement of the GS_P is not shown.

polarizing elements used can be completely, simultaneously determined [13].

From the above argument, it is found that a sophisticated apparatus needs six fully independent drive shafts (η, ω, θ, χ, φ, and ψ). If so, it allows us to perform not only conventional reflection measurements (two-dimensional scans ω-θ and φ-ψ, where θ and ψ are fixed at 2ω and 2φ, respectively) but also one-dimensional scans such as rocking curve and transmission measurements. Furthermore, it is convenient to adjust the angular alignment between the optical axis and the sample position.

3. Design and construction of a soft x-ray polarimeter and ellipsometer

Figure 2 shows the projection drawing (a) and photograph (b) of the internal mechanism, and photograph of the vacuum chamber (c), of a soft x-ray polarimeter and ellipsometer (SXPE) for complete polarization analysis which we have developed [8, 9]. This consists of two goniometric stages GS_P and GS_A to be able to mount a phase shifter (or polarizer) P and an analyzer A, respectively, and is equipped with six motorized rotary stages (χ, ψ, φ, η, θ, and ω) to realize the configurations as shown in Fig. 1, and three motorized linear stages (H, X, and T) as auxiliary drive shafts to adjust the positions of P, A, and the internal mechanism itself. All motorized stages are made by Suruga Seiki Co., Ltd., Japan, the details of which are listed in Table 1.

The GS_P has three rotary stages (χ, ψ, and φ) and two linear stages (H and T). The azimuth rotation of GS_P is operated by the χ stage connected to a rectangular frame made of aluminum alloy supported by a U-shaped basement with a bearing. The ψ stage on the U-shaped arm with a bearing shaft is used for moving the position of GS_A. A counter weight made of stainless steel is attached on the opposite side of GS_A. The φ stage can change the incident angle of P. The height position of P can be changed by the H stage connected just below the φ stage. The T stage located just below the bottom plate of the U-shaped basement of the GS_P (not shown in the figure) is used to move the internal mechanism parallel to the *x* direction, where *x* is normal to the surface of the sample.

The GS_A is connected to the arm on the ψ stage and is composed of three rotary stages (η, θ, and ω) and a linear stage (X). The azimuth rotation of GS_A is operated by the η stage. The incident angle of A can be changed by the ω stage located on the X stage for moving and

Table 1 Details of the motorized stages assigned to the drive shafts of the goniometric stages GS_A and GS_P. The resolution per pulse of each axis is a nominal value in the atmosphere.

Stage	Symbol of axis	Annotation of axis	Operation range	Resolution per pulse	Motorized stage
GS_A	η	Azimuth angle of A	–5 ~ 370°	0.00125°	U10698
	ω	Incident angle of A	–5 ~ 180°	0.001°	KS401-60-L
	θ	Angle of detector arm	–5 ~ 120°	0.001°	KS401-60-L
	X	Height position of A	–5 ~ 5 mm	0.5 μm	KS101-20-L
GS_P	χ	Azimuth angle of P	–5 ~ 370°	0.001°	KS402-100-L
	φ	Incident angle of P	–5 ~ 180°	0.001°	KS401-60-L
	ψ	Angle of arm	–5 ~ 120°	0.001°	KS402-100-L
	H	Height position of P	–5 ~ 5 mm	0.5 μm	KS101-20-L
	T	Horizontal position of the internal mechanism	–15 ~ 15 mm	1.0 μm	KX0830C-L-L

adjusting the height position of A, where the ω and X stages are the same specifications as the φ and H stages of GS_P, respectively. The θ stages are used for changing the detector arm where a microchannel plate (MCP) assembly (F4655CsI, Hamamatsu Photonics K.K.) with an 18-mm outer diameter and a 14.5-mm effective detection area is attached. MCP's satisfies the demands of high efficiency but low dark current along with low polarization sensitivity. Also the assembly that we have employed is light and compact, so that it can reduce loads on the motorized stages.

The sample holder for P and its holder housing are the same specifications as those for A. A sample having a size of up to 15 × 15 × 5 mm^3 can be mounted on this holder. Each back plate of the holder and its housing has a 5-mm diameter hole. Therefore, transmission experiment for A (or P) can be also performed by detaching P (or A) from the light source by means of the H (or X) stage. Furthermore, the rotor shaft that supports the rectangular frame of GS_P has a 2-mm pinhole (see Fig. 2(a)). The 0-th order light from the monochromator can be observed directly via this pinhole when both P and A are detached from the optical axis, so that it is easy to realize not only the configurations as shown in Fig. 1 but also transmission geometries and the position alignment.

The vacuum chamber made of a stainless steel is a cylindrical tube with an 845-mm diameter and an

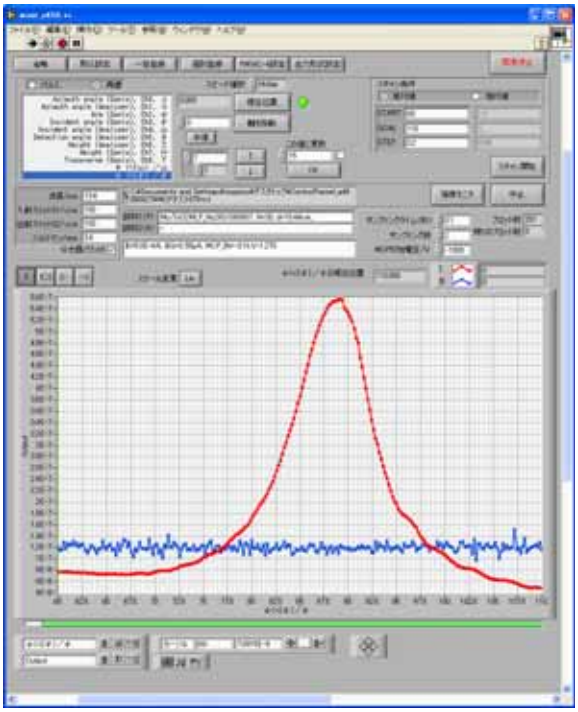

Figure 3 Newly developed LabVIEW® based program. This allows us to do adjustment of each axis as well as several one- and two- dimensional scans, e.g., polarization measurements based on rotating-analyzer ellipsometry (χ- and η- scans), rocking-curve and transmission measurements (φ- and ω- scans), and conventional reflection measurements (ψ/φ- and θ/ω- scans, where ψ and θ are fixed at 2φ and 2ω, respectively).

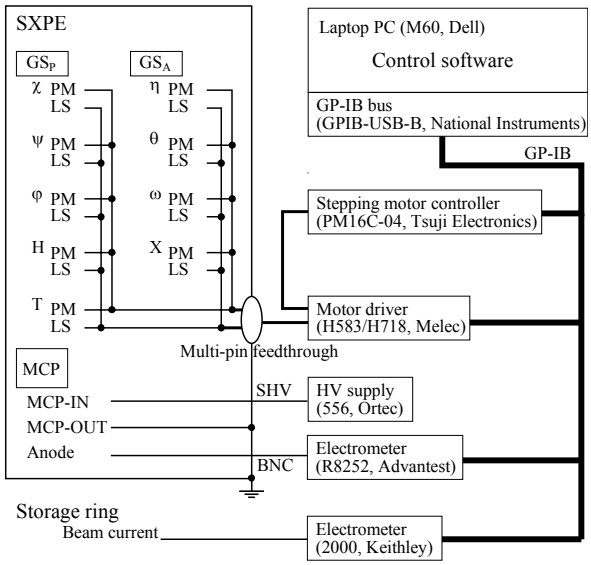

Figure 4 Block diagram of the control system of SXPE. PM and LS mean pulse motor and limit sensor of the motorized stage, respectively.

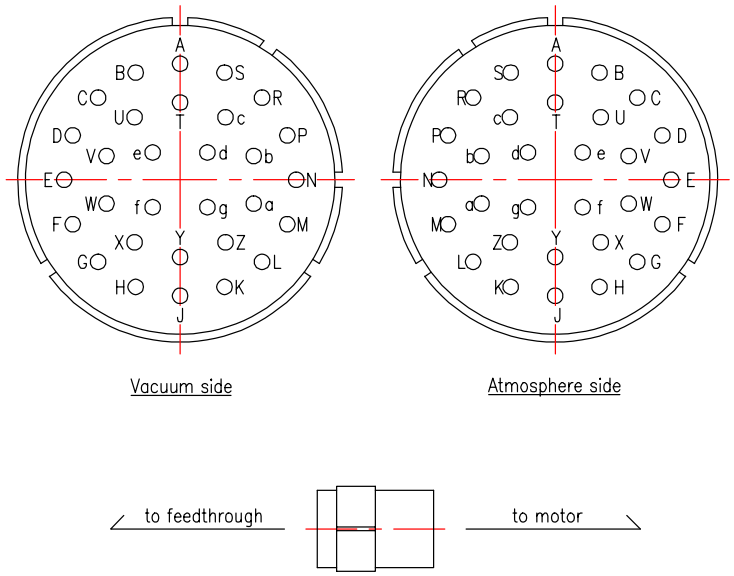

Symbol	Assignment	Color	Connector label			
			index	A	B	C
A	Motor lead (Black)	Black	1	χ	ω	φ
B	Motor lead (Green)	Green				
C	Motor lead (Orange)	Orange				
D	Motor lead (Red)	Red				
E	Motor lead (Blue)	Blue				
F	CWLS Out	Brown				
G	CCWLS Out	Yellow				
H	ORG In	Gray				
J	DC5V (+)	Violet				
K	DC5V (-)	White				
L	Motor lead (Black)	Black	2	η	θ	ψ
M	Motor lead (Green)	Green				
N	Motor lead (Orange)	Orange				
P	Motor lead (Red)	Red				
R	Motor lead (Blue)	Blue				
S	CWLS Out	Brown				
T	CCWLS Out	Yellow				
U	ORG In	Gray				
V	DC5V (+)	Violet				
W	DC5V (-)	White				
X	Motor lead (Black)	Black	3	T	X	H
Y	Motor lead (Green)	Green				
Z	Motor lead (Orange)	Orange				
a	Motor lead (Red)	Red				
b	Motor lead (Blue)	Blue				
c	CWLS Out	Brown				
d	CCWLS Out	Yellow				
e	ORG In	Gray				
f	DC5V (+)	Violet				
g	DC5V (-)	White				

Figure 5 Connector pin assignment of a 30-pin electrical feedthrough. The axes of χ, η, T, ω, θ, X, φ, ψ, and H are assigned to connector labels of A1, A2, A3, B1, B2, B3, C1, C2, and C3, respectively.

800-mm total length (see Fig. 2(c)). A base pressure of 8×10^{-5} Pa is achieved using a turbo molecular pump of 800-L/s and a scroll pump of 1000-L/min. A four-quadrant slit located upstream of this chamber is equipped to form an incoming beam.

A control software has been also developed with LabVIEW® published by National Instruments along with the apparatus (Fig. 3). This allows us to do adjustment of each axis as well as several one- and two- dimensional scans, e.g., (1) polarization measurements based on rotating-analyzer ellipsometry (χ- and η- scans in double- reflection and transmission geometries, and reflection-transmission geometry and vise versa), (2) rocking-curve and transmission measurements (φ- and ω- scans), (3) conventional reflection measurements (ψ/φ- and θ/ω- scans, where ψ and θ are fixed at 2φ and 2ω, respectively), and (4) time dependence of the beam intensity. Figure 4 shows a block diagram of the control system of the apparatus. All connection wires of nine motorized stages are connected to nine stepping motor drivers (H583 and H718, Melec Inc.) through three 30-pin electrical feedthroughs, of which the connector pin assignment is described in Fig. 5. Three 30-pin electrical feedthroughs are compatible specifications each other. One feedthrough connects three motorized stages. A*i*, B*i*, and C*i* (*i* = 1, 2, 3) in the assignment table mean the respective feedthroughs. The wires driving χ, η, T, ω, θ, X, φ, ψ, and H are connected to the connector labels of A1, A2, A3, B1, B2, B3, C1, C2, and C3, respectively. Nine motor drivers are controlled by a stepping motor controller (PM16C-04, Tsuji Electronics Co., Ltd.) via a GPIB bus (GPIB-USB-B, National Instruments Co.). The signal from the anode of the MCP is read out by an electrometer (R8252, Advantest Co.), whose noise level is lower than 0.3 pA. Another electrometer (Model 2000, Keithley Instruments Inc.) is used to monitor the beam current of the storage ring. They are automatically recorded in comma separated value (CSV) file format in every measurement. Only a high-voltage supply (556, Ortec) applied to the MCP detector is manually driven.

4. Sample preparation

A Mo/Si multilayer mirror was optimized at a wavelength of 13.9 nm and fabricated for the purpose of use as a polarizer in the performance test of the new apparatus. The Mo/Si multilayer sample was deposited on the surface of a commercial Si(111) substrate with a 2-inch diameter and an 1-mm thickness at ambient temperature using an ion beam sputtering method. The base pressure was lower than 8×10^{-6} Pa and the Ar gas pressure was fixed at 0.016 Pa while the deposition. The Mo/Si multilayer was grown to 23 bilayers with topmost Si layer. The deposition rates were 0.0588 nm/s and 0.0356 nm/s for Mo and Si layers, respectively.

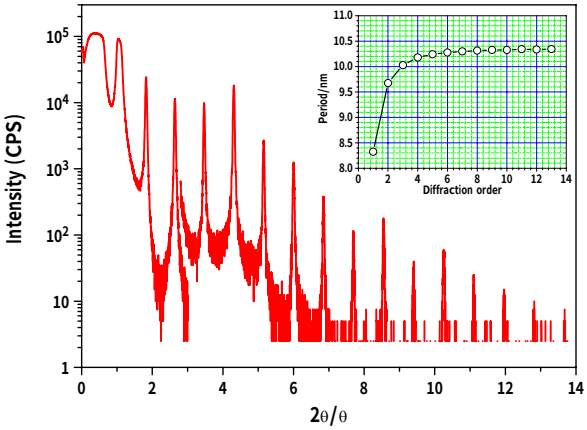

Figure 6 X-ray diffraction profile of the Mo/Si multilayer. The inset means the periodic length of the multilayer estimated from peak position in each diffraction order.

Figure 6 shows the x-ray diffraction profile of the Mo/Si multilayer examined by a high-resolution x-ray diffractometer (SLX-2000, Rigaku Co.) using Cu-K_α (0.154 nm) emission line. Sharp and intense Bragg peaks were observed. From the relation between the peak position and diffraction order, the periodic length and the ratio of the Mo layer thickness to the multilayer period were evaluated to be 10.36 nm and 0.64, respectively.

The fabricated multilayer mirror was cut into half size pieces. One was used for the reflection measurement using an existing conventional reflectometer. The details are described below. The other was also cut into three pieces having an equal size of 15×15 mm^2. Two of those specimens were used as a polarizer and analyzer in the performance test.

5. Experimental

The soft x-ray polarimeter and ellipsometer (SXPE) for complete polarization analysis has been installed at the end station of the soft x-ray beamline (BL-11) of AURORA, a superconducting compact storage ring,[12] at SR Center of Ritsumeikan University. The major machine parameters of AURORA are as follows: electron energy = 575 MeV; orbital

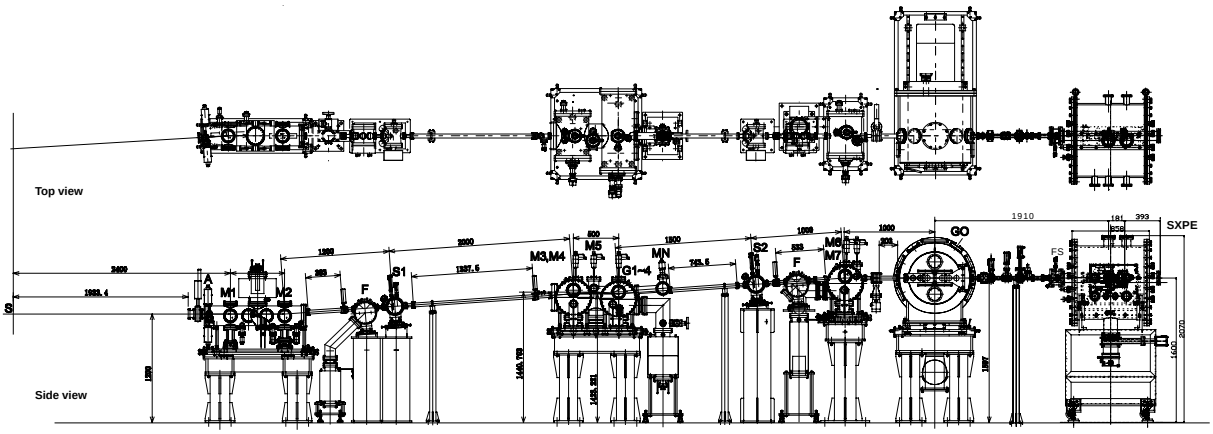

Figure 7 Top and side views of BL-11 where SXPE is installed at the back of the end station.

radius = 1.0 m; critical wavelength λ_c = 1.5 nm; electron beam current = 300 mA; horizontal beam size σ_y = 1.3 mm; vertical beam size σ_z = 0.14 mm; brightness = 1.8×10^{12} photons/s/mm^2/mrad^2/0.1% bandwidth at 4.5 nm.

Figure 7 shows the top and side views of BL-11 where SXPE is installed at the back of the end station. BL-11 [11, 15] is an evaluation beamline for soft x-ray (SX) optical elements, e.g., thin films, multilayer mirrors, gratings, and crystals, which consists of prefocus system, monochromator system, reflectometer system, and control system. The prefocus system comprises beam-shaping apertures A and focusing mirrors M1 and M2. The maximum acceptance angles determined by these apertures are 5 mrad (*H*) × 3 mrad (*V*). The monochromator system consists of two types of grazing incidence Monk-Gillieson (M-G) monochromators in order to cover a wavelength range between 0.6 nm and 25 nm. One is a conventional M-G monochromator equipped with three laminar-type varied-line-spacing (VLS) holographic gratings G1 (300 lines/mm), G2 (600 lines/mm), and G3 (1200 lines/mm). [16] These gratings can be used interchangeably at an included angle of either 176° or 172°, depending on a required wavelength scanning range. One particular included angle is easily selected by inserting the vertical focusing spherical mirror M3 or M5 into the beam at the angle of incidence of 88° or 86°. This monochromator covers the wavelength range of 1.2-25 nm. The other monochromator is a new type that employs a scanning mechanism based on surface normal rotation (SNR) of the grating G4 (600 lines/mm).[17, 18] It covers the wavelength range of approximately 0.6-2 nm. The reflectometer system consists of filters F (thin films of B, C Al, Si, Ti, Cr, and Fe), post-focusing toroidal mirrors M6 and M7, and a modified θ-2θ reflectometer/diffractometer (MRD), indicated by GO in Fig. 7. A glass window gate valve in front of the four-quadrant slit FS that separates MRD and SXPE makes it easy to align SXPE with the optical axis because the 0-th order light from the monochromator of BL-11 can be observed through this window even if the chamber of SXPE is vented to atmosphere.

In this study, the beam-shaping apertures A of BL-11 were set to 5 mm (*H*) × 1.5 mm (*V*). The acceptance angles were estimated to be 3 mrad (*H*) × 1 mrad (*V*). Also, the conventional M-G monochromator mode with the laminar-type VLS holographic grating G1 and the mirror M5 was chosen because it was suitable for polarization measurement with Mo/Si multilayer polarizers at around 100 eV. A thin Si film of ~0.5 μm thickness located after the exit slit was used to reduce unwanted higher order light. In the conventional reflection measurement by MRD, the post-focusing toroidal mirror M6 was chosen, which gives focus onto a sample placed in MRD. On the other hand, in the reflection and linear polarization measurements by SXPE, the post-focusing toroidal mirror was replaced from M6 to M7. Unfortunately, M7 provides focus at a point 150 mm downstream from the back flange of the MRD chamber. Thus, an incoming beam to the polarizer in SXPE was defocused. Therefore, the beam dimension was limited to 1 × 1 mm^2 by FS set just in front of the SXPE chamber. The beam size at the detector equipped in SXPE was slightly smaller than 2 × 2 mm^2, where it was checked by white light from the monochromator. From this result, the divergence of approximately 2 mrad was estimated.

The polarization measurement based on the rotating-analyzer method as shown in Fig. 1 was performed in a wavelength range of 12.4 -14.8 nm. The incident wavelength was changed by the control system of BL-11. The angles of incidence of both the Mo/Si multilayers, P and A, in SXPE were scanned from 37.5° to 52.3° by the control program (see Fig. 3). When the

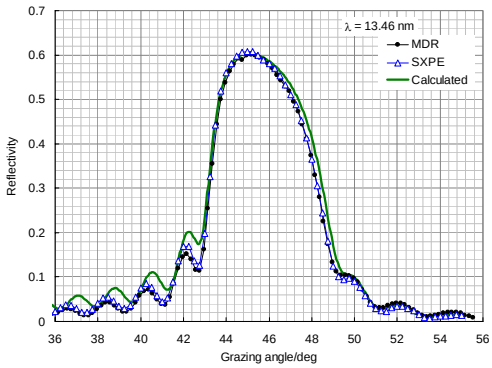

Figure 8 Reflectivities for s-polarization of the Mo/Si multilayers measured by SXPE (open circles) and MRD (solid squares) at 92 eV as a function of the grazing angle. Solid line stands for the calculated curve under the assumption of a Debye-Waller factor of a 0.5-nm rms interfacial roughness.

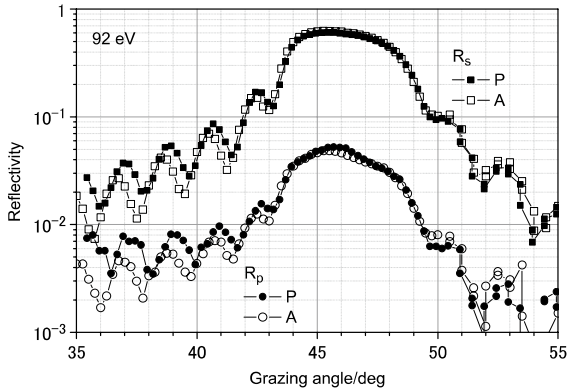

Figure 9 Reflection profiles for s- and p-polarization components (R_s and R_p) of the Mo/Si multilayer polarizer and analyzer measured by SXPE at an energy of 92 eV as a function of the grazing angle, where the vertical axis is in logarithmic scale.

exit slit width of the monochromator was set to 300 μm, the resolving power was estimated to be approximately 100.

6. **Performance test**

Figure 8 shows the reflectivity for s-polarization of the Mo/Si multilayer measured by SXPE in the configuration in Fig. 1(b) at an incident energy of 92 eV as a function of the grazing angle, indicated by open circles. Solid squares represent the reflection profile for s-polarization measured by MRD. For the reference, the calculated curve under the assumption of a Debye-Waller factor [19] of a 0.5-nm rms interfacial roughness is also shown in this figure by solid line. The efficiency, reflection width, and peak position measured by SXPE are in good agreement with those by MRD. This means SXPE has satisfactory performance as a conventional reflectometer. The calculated curve deviates from the experimental data in the small angle region but it is kind of important because the disagreement between the measured and calculated curves would be improved by modifying the model of the multilayer structure.

Figure 9 shows both reflection curves for s- and p-polarization components of the Mo/Si multilayer polarizer and analyzer mounted in SXPE at the incident energy of 92 eV, where the abscissa axis means the angles of incidence (φ for the polarizer and ω for the analyzer) and the vertical axis is in logarithmic scale. The reflectivity for s- (or p-) polarization R_s (or R_p) of the analyzer is evaluated to be 62% (or 4.8%) at the angle of incidence of 45.75°, whose full width at half maximum (FWHM) is about 4°. These values agreed well with those of the polarizer. It is reasonable because the multilayers used as the polarizer and analyzer cut out from the same specimen. Nevertheless, both reflection curves could not be completely identical. The slight difference between the reflection curves in the region deviating from the main peaks is considered to be the effect of a difference of the distances from the position of the detector to the polarizer and to the analyzer.

The above result shows that the reflectivities for the individual polarized light can be evaluated quantitatively by using SXPE. It is, however, impossible to determine the degree of

linear polarization of the probe light from only the above experiment as well as the polarizances of the polarizer and analyzer, as described in Section 2.

Figure 10 shows the azimuth angle dependences of reflection intensities obtained in the three configurations in Fig. 1 at the energy of 92 eV (solid circles). The azimuth angles χ and η are measured clockwise to an observer from the horizontal plane. The sets of solid circles indicated by (a), (b), and (c) correspond to the configurations in Figs. 1(a), (b), and (c), respectively. The vertical axis is in logarithmic scale. The incident angles of the polarizer and the analyzer were fixed at 45.75°. Solid lines in this figure stand for the results of the curve-fitting analysis and they are in good agreement with the respective measured data. Consequently, the fitting parameters C_i and δ_i (i = 1, 2, 3) have been determined, whose values are listed in Table 2. In fact, the values of C_3 and δ_3 can be obtained in equivalent geometries to the azimuth angle $\chi = \delta - \pi/4$ of P, i.e., $\chi = \delta + (2n - 1)\pi/4$ (n = 0, 1, 2, 3). Substituting them into Eq. (5), we obtain $P_L = 0.872 \pm 0.007$ as an average of four equivalent geometries. From this, Eq. (4) yields $Z_1 = 0.979 \pm 0.008$ for the analyzer and $Z_2 = 0.960 \pm 0.008$ for the polarizer. The polarizance of A (P) and the degree of linear polarization of light were demonstrated to be able to determine simultaneously. In addition, some remaining parameters such as P, P_C, and ε of light, and ρ and Δ of the phase shifter, as well as those of the analyzer, can be in principle determined by applying Eq. (6) to the four (χ, η_3) pairs, that is, it is the procedure for complete polarization analysis. However, it would

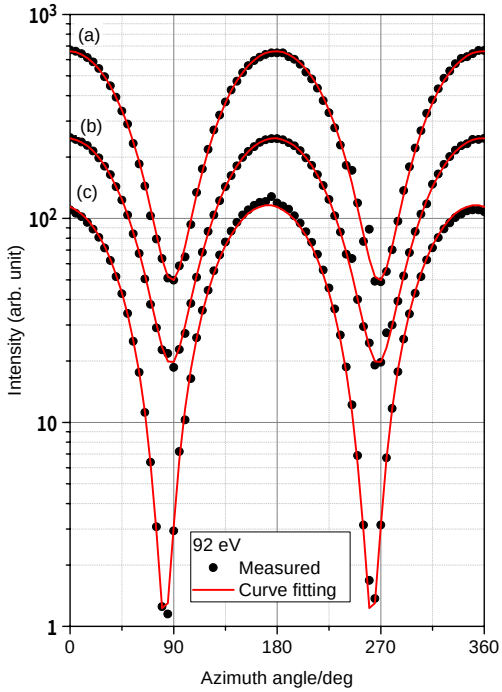

Figure 10 Azimuth angle dependencies of reflection intensities at 92 eV. The azimuth angles χ and η are measured clockwise to an observer from the horizontal plane. The sets indicated by (a), (b), and (c) show the measured values in the configurations shown in Figs. 1(a), (b), and (c), respectively. The results of the curve-fitting analysis are shown by solid lines. The vertical axis is in logarithmic scale.

Table 2 Results of curve-fitting analysis associated with Fig. 10. The values of C_3 and δ_3 were obtained at the azimuth angle $\chi = \delta + (2n - 1)\pi/4$ (n = 0, 1, 2, 3). Z_1 and Z_2 were derived from the average value $P_L = 0.872 \pm 0.007$.

Configuration (a)		C_1	δ_1	Z_1
		0.854 ± 0.002	–2.42 ± 0.14	0.979 ± 0.008
Configuration (b)		C_2	δ_2	Z_2
		0.837 ± 0.002	–1.74 ± 0.12	0.960 ± 0.008
Configuration (c)		C_3	δ_3	P_L
n	0	0.953 ± 0.008	–7.71 ± 0.79	0.882 ± 0.009
	1	0.951 ± 0.002	0.54 ± 0.24	0.867 ± 0.003
	2	0.982 ± 0.001	–7.71 ± 0.17	0.869 ± 0.003
	3	0.943 ± 0.003	0.43 ± 0.24	0.871 ± 0.003

need more data to avoid being trapped in local minimum. The Mo/Si multilayers prepared were found to work as high-performance polarizers. Although there exists a slight difference between Z_1 and Z_2, it is thought to be caused by the difference of the distance from each polarizing element to the detector, backlash of the mechanism, the non-uniformity of the detector response, and/or etc. Also the value of P_L seems to be somewhat small in spite of SR from a bending magnet. The phenomenon is supposed to be caused by an inhomogeneous mixture of left and right handed helicities of the bending magnet source or a depolarization effect from reflection and diffraction by the beamline optics. This should be examined in detail in the future.

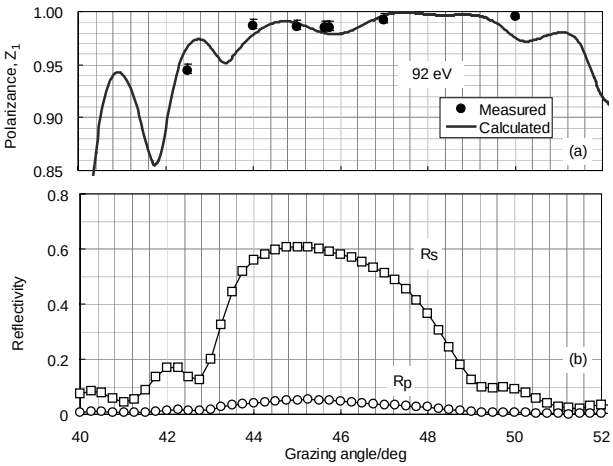

Figure 11 Incident angle dependence of the polarizance Z_1 (a) and measured reflectivities for s- and p-polarization (b) of A at 92 eV. The calculated curve of the polarizance is indicated by solid line.

In addition, the polarizance Z_1 (or Z_2) of A (or P) at an arbitrary angle of incidence can be evaluated by only the contrast factor of the probe light because the value of P_L has already been determined above. Figure 11(a) shows the incident angle dependence of the polarizance Z_1 of A at 92 eV. The calculated curve is also indicated by solid line. For the reference, measured reflectances for s- and p-polarization (R_s and R_p) of A are shown by open squares and open circles, respectively in Fig. 11(b). The values of Z_1 in the vicinity of the main peak of R_s were evaluated to be above 97%, and they agreed with the calculated value. It is because that the polarizance Z is independent on only the respective values of R_s and R_p as seen from Eq. (3), although R_s and R_p are significantly affected by a Debye-Waller factor. Hence, the value of P_L determined by the above experiment can be considered as sufficiently reliable.

Figure 12 shows the wavelength dependences of the linear polarization degree P_L and azimuth angle δ of the incident light, and the polarizance Z_1 (or Z_2) of A (or P), in the wavelength range from 12.4 nm to 14.8 nm, where the value of P_L, as well as Z_i (i = 1, 2), were calculated as an average of four equivalent geometries to the azimuth angle $\chi = \delta - 45°$ of P, i.e., $\chi = \delta + (2n - 1) \times 45°$ (n = 0, 1, 2, 3), in Fig. 1(a), where the χ is measured clockwise to an observer from the horizontal plane. It is found that P_L and δ are almost constant with P_L = 85-88% and $|\delta|$ = 0.5°-1.5°. This is the first experimental result on the wavelength dependence of the linear polarization degree at BL-11 and is useful for the efficiency correction of SX optical elements such as multilayer mirrors and gratings (including multilayered gratings) by means of MRD. From the theoretical calculation the linear polarization degree is anticipated to be approximately 90% at the exit port of the storage ring assuming the vertical acceptance angle of 1 mrad.[20] Therefore the experimental data is in good agreement with the calculation. A slight difference between the calculated and measured P_L is thought to be caused by an inhomogeneous mixture of left and right handed helicities of the bending magnet source or a depolarization effect from reflection and diffraction by the beamline optics. This should be examined in detail in the future. On the

other hand, Z_i is strongly dependent on the wavelength and has a peak of over 99% at around 14 nm. This is reasonable because the prepared multilayer has been designed and fabricated as a polarizer for 13.9 nm radiation. Also, a slight inconsistency between Z_1 and Z_2 may be attributed to the difference of the distances from the position of the detector to P and to A, the backlash of the drive mechanism, and/or the non-uniformity of the detector response, etc.

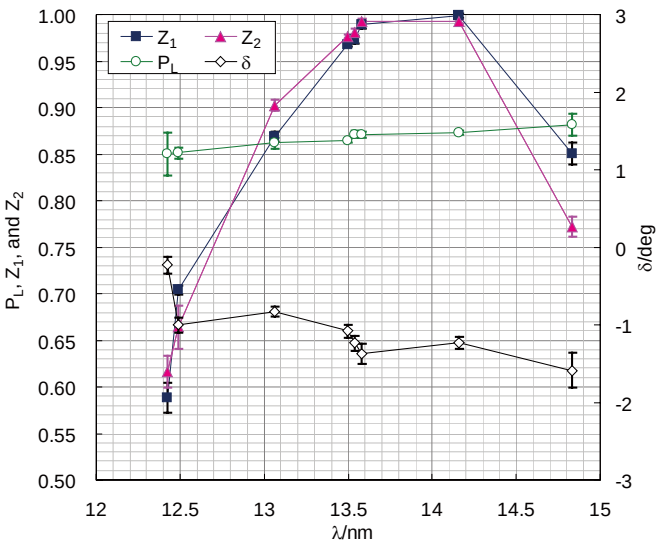

Figure 12 Plots of the linear polarization degree, P_L, and the azimuth angle, δ, of the major axis of the polarization ellipse, of the incident light, and the polarizances Z_i of A and P vs. the wavelength λ. The azimuth is measured clockwise with respect to an observer from the horizontal plane.

At this point, some polarization parameters of the light, i.e., the circular polarization degree P_C and the ellipticity angle ε have not been determined yet. As a next subject, we will pursue to fabricate a phase shifter usable in the same energy range as the analyzer and perform the complete polarization analysis. Nevertheless, it is very meaningful that the value of P_L of the monochromatized SR beam from BL-11 has been evaluated quantitatively for the first time since the construction of the beamline. Also, it is concluded that SXPE has completed with satisfactory performance as the polarimeter and ellipsometer in the SX region, as well as BL-11 is upgraded as the comprehensive evaluation beamline for optical elements including polarizing elements.

Summary

A new apparatus to perform polarimetric and ellipsometric measurements based on the rotating-analyzer ellipsometry in the SX region has been designed, constructed, and installed in the SX beamline (BL-11) at SR Center of Ritsumeikan University. It can realize the optical configurations of two polarizing elements required for complete polarization analysis by means of six independently movable drive shafts. As a demonstration of this apparatus, linear polarization measurement in the wavelength range of 12.4-14.8 nm has been carried out at BL-11 by using two Mo/Si multilayer polarizers deposited by an ion beam sputtering method. As the result, the degree of linear polarization of BL-11 has been determined to be 85-88% in the measured wavelength range for the first time since the construction of the beamline, as well as the polarization characteristics of two polarizers used have been evaluated, best performance of which are the polarizances of over 99% and the s-polarized reflectances of 62% in the vicinity of 13.9 nm.

In this study, we focused on the polarization measurement with only the reflection-type polarizer and analyzer and verified the degree of linear polarization of light but did not use transmission-types or a phase shifter. Nevertheless, the degree of circular polarization can be evaluated in the same manner as the above procedure only if the polarizer is replaced by a

phase shifter. Therefore our newly developed apparatus has the capability to perform the complete polarimetric and ellipsometric measurements in the SX region. Taking advantage of this, complete polarization analysis in the various energy ranges and the characteristics of polarizing elements would be performed at BL-11.

Acknowledgement

We would like to thank Dr. H. Kimura of SPring-8, Japan Synchrotron Radiation Research Institute for his fruitful discussion. We wish to thank Prof. T. Ohta and his staff of SR Center, Ritsumeikan University for their technical support.

References

[1] T. Koide, T. Shidara, M. Yuri, N. Kandaka, K. Yamaguchi, and H. Fukutani, Nucl. Instr. Meth. Phys. Res. A 308, 635-644 (1991).
[2] F. Schäfers, H.-C. Mertins, A. Gaupp, W. Gudat, M. Mertin, I. Packe, F. Schmolla, S. D. Fonzo, G. Soullié, W. Jark, R. Walker, X. L. Cann, R. Nyholm, and M. Eriksson, Appl. Opt. 38, 4074-4088 (1999).
[3] M. A. MacDonald, F. Schäefers, R. Pohl, I. B. Poole, A. Gaupp, and F. M. Quinn, Rev. Sci. Instrum. 79, 025108 (2008).
[4] K. Hirano, T. Ishikawa, I. Nakamura, M. Mizutani, and S. Kikuta, Jpn. J. Appl. Phys. 33, L689-L692 (1994).
[5] T. Imazono, M. Ishino, M. Koike, H. Kimura, T. Hirono, and K. Sano, Rev. Sci. Instrum. 76, 023104 (2005).
[6] T. Imazono, T. Hirono, H. Kimura, Y. Saitoh, Y. Muramatsu, M. Ishino, M. Koike, and K. Sano, Rev. Sci. Instrum. 76, 126106 (2005).
[7] H. Kimura, T. Hirono, T. Miyahara, M. Yamamoto, and T. Ishikawa, AIP Conf. Proc. 705, 537-540 (2004).
[8] T. Imazono and M. Koike, AIP Conf. Proc. 879, 690-693 (2007).
[9] T. Imazono, K. Sano, Y. Suzuki, T. Kawachi, and M. Koike, Rev. Sci. Instrum. 80, 085109 (2009).
[10] T. Imazono, Y. Suzuki, K. Sano, and M. Koike, Spectrochimica Acta B. 65, 147-151 (2010).
[11] M. Koike, K. Sano, Y. Harada, O. Yoda, M. Ishino, K. Tamura, K. Yamashita, N. Moriya, H. Sasai, M. Jinno, and T. Namioka, Proc. SPIE 4782, 300-307 (2002).
[12] H. Iwasaki, Y. Nakayama, K. Ozutsumi, Y. Yamamoto, Y. Tokunaga, H. Saisho, T. Matsubara, and S. Ikeda, J. Synchr. Rad. 5, 1162-1165 (1998).
[13] H. Kimura, Doctoral thesis, The Graduate University for Advanced Studies, Japan (1992).
[14] T. Imazono, K. Sano, Y. Suzuki, T. Kawachi, and M. Koike, AIP CP (SRI2009) (in press).
[15] M. Koike, K. Sano, O. Yoda, Y. Harada, M. Ishino, N. Moriya, H. Sasai, H. Takenaka, E. Gullikson, S. Mrowka, M. Jinno, Y. Ueno, J. H. Underwood, and T. Namioka, Rev. Sci. Instrum. 73, 1541-1544 (2002).
[16] M. Koike and T. Namioka, Appl. Opt. 36, 6308-6318 (1997).
[17] M. C. Hettrick, Appl. Opt. 31, 7174-7178 (1992).
[18] M. Koike and T. Namioka, Appl. Opt. 41, 245-257 (2002).
[19] E. Spiller, Soft X-ray Optics (SPIE, Seattle, 1994), pp. 111-114.
[20] T. Ohta (private communication).